Pramana – J. Phys. (2017) 89:21
DOI 10.1007/s12043-017-1411-2

Electro-optic response of metal halide $CsPbI_3$: A first-principles study

AMREEN BANO*, PREETI KHARE and N K GAUR

Department of Physics, Barkatullah University, Bhopal 462 026, India
*Corresponding author. E-mail: banoamreen.7@gmail.com

MS received 13 June 2016; revised 29 December 2016; accepted 25 January 2017; published online 8 July 2017

Abstract. A theoretical study of electronic and optical properties of metal-halide cubic perovskite, $CsPbI_3$, is presented, using first-principles calculations with plane-wave pseudopotential method as implemented in the PWSCF code. In this approach, local density approximation (LDA) is used for exchange-correlation potential. A strong ionic bonding is observed between Cs and I orbitals and a weak covalent bonding is found between Pb-I and Cs-Pb orbitals. The optical properties of this compound are interesting and it has many applications in optoelectronic devices.

Keywords. Electronic band structure; density of states; dielectric function; refractive index; absorption coefficient; optical conductivity.

PACS Nos 71.20.−b; 78.20.ci

1. Introduction

The family of perovskite crystals (ABX_3) is an interesting class of materials which exhibit a vast range of physical properties like, high thermoelectric power, ferroelectricity, charge-ordering, superconductivity, spin-dependent transport, colossal magnetoresistance (CMR) [1–3] etc. The studies of organometal halide perovskites for their applications in photovoltaic devices have taken a giant leap over the last 5–6 years [4]. These studies are motivated by the goal of fabricating stable, high efficiency and cost effective solid-state solar cells [5]. Advanced hybrid perovskite materials like $CsPbI_3$ have found extensive applications as solar cell absorbers, topological insulators, superconductors etc. [6,7]. On the other hand, oxide perovskites (ABO_3) are formed from divalent A^{II} (1b site – cuboctahedral) and tetravalent B^{IV} (1a site – octahedral) metals and halide perovskites e.g. (ABI_3) can be formed from monovalent A and divalent B metals. In the case of conductors, the compounds are exclusively oxides, whereas the halides are insulators in general, except the lead–iodine system. Several strategies have been adopted to increase the power conversion efficiencies of halide perovskites, some targeting the quality of perovskite films, e.g. its uniformity [8], others focussing on their intrinsic optical and electronic properties such as tuning of band gap E_g [9,10]. In the latter case, the objective is to obtain a compound with a band gap close to the ideal value of 1.1 eV.

The $CsPbI_3$ crystal belongs to an interesting class of semiconducting perovskite which is currently used in thin-film field-effect transistor made of organic–inorganic hybrid compounds. The benefit of using hybrid compounds resides in their ability to combine the advantage of these two classes of compounds: the high mobility of inorganic materials and the ease of processing of organic materials [11,12]. In spite of the growing attention towards this new material, very little attention has been paid to the electronic and optical properties of the inorganic part of these compounds. To the best of our knowledge, no attempts have been made to study the optical properties of cubic $CsPbI_3$. In this paper, we assess the properties of halide perovskite $CsPbI_3$ using density functional theory (DFT) for ground-state properties like electronic band structure, and density functional perturbation theory (DFPT) for dielectric and optical response functions. We have provided the insights into the key properties required for device models that underpin their utility in optical and optoelectronics.

2. Computational details

The first-principles calculations of $CsPbI_3$ are performed within the framework of density functional

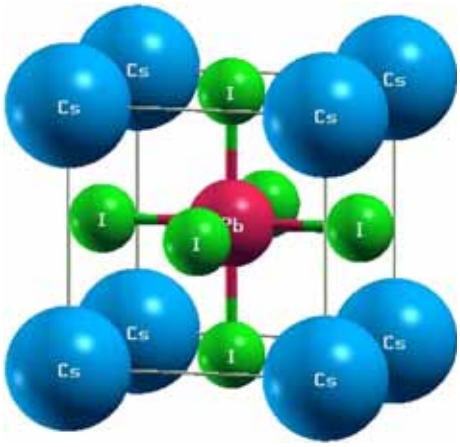

Figure 1. The unit cell of cubic $CsPbI_3$.

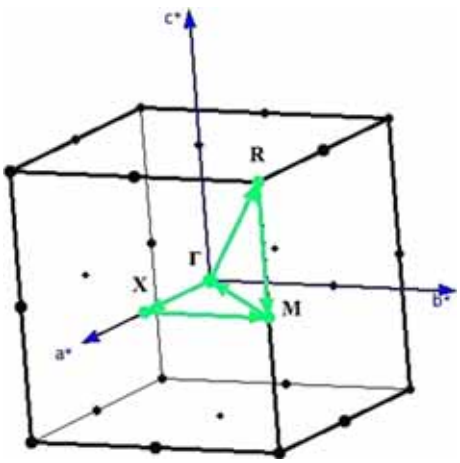

Figure 2. Brillouin zone corresponding to cubic $CsPbI_3$.

theory (DFT) using plane-wave pseudopotential method as implemented in PWSCF code [13]. The exchange-correlation potential is determined with LDA of Perdew and Zunger [14–16]. The dependence of total energy on the number of K-points in the irreducible wedge of Brillouin zone (BZ) has been explored by performing calculations for $6 \times 6 \times 6$ Monkhorst-Pack K-mesh for energy convergence. The optical properties are studied by using epsilon.x which is a post processing code of PWSCF [13], at Γ point [17,18]. The unit cell has five atoms and their positions were raised within the framework of cubic ($Pm3m$) structure. The unit cell of cubic $CsPbI_3$ can be seen in figure 1.

The Kohn–Sham orbitals are described by a plane-wave basis set with a kinetic energy cut-off of 30 Ry [17,19,20]. The electronic band structure is calculated along high symmetry directions in the BZ (Γ(0, 0, 0); X(0.5, 0, 0); M(0.5, 0.5, 0); Γ(0, 0, 0); R(0.5, 0.5, 0.5)) with DFT approach [21], that can be seen in figure 2. The optical response of $CsPbI_3$ is described by the frequency-dependent dielectric function as

$$\varepsilon(\omega) = \varepsilon_1(\omega) + i\varepsilon_2(\omega), \tag{1}$$

where $\varepsilon_1(\omega)$ and $\varepsilon_2(\omega)$ are the real and imaginary parts of the dielectric function $\varepsilon(\omega)$ [6,13,16]:

$$\varepsilon_1(\omega) = 1 + \frac{2}{\pi} P \int_0^\infty \frac{\omega' \varepsilon_2(\omega') \mathrm{d}\omega'}{\omega'^2 - \omega^2} \tag{2}$$

and

$$\varepsilon_2(\omega) = \left(\frac{4\pi^2 e^2}{m^2\omega^2}\right) \sum_{i,j} \int_k \langle i|M|j\rangle^2 f_i(1 - f_i) \times \delta^k(E_{j,k} - E_{i,k} - \omega)\mathrm{d}^3k. \tag{3}$$

Here, P denotes the principle part of the integral, e is the polarization vector of the electric field, M is the dipole matrix, i and j are the initial and final states respectively, f_i is the Fermi distribution function for the ith state and E_i is the energy of the electron in the ith state with crystal wave vector **k**. The energy loss function $L(\omega)$ is given as [15,16,22]

$$L(\omega) = \mathrm{Im}\left(-\frac{1}{\varepsilon(\omega)}\right). \tag{4}$$

Real and imaginary parts of the dielectric function are used to calculate refractive index $\eta(\omega)$ and extinction coefficient $\kappa(\omega)$ using the following relations:

$$\eta(\omega) = \frac{1}{\sqrt{2}}\left[\left\{\epsilon_1(\omega)^2 + \epsilon_2(\omega)^2\right\}^{1/2} + \epsilon_1(\omega)\right]^{1/2} \tag{5}$$

and

$$\kappa(\omega) = \frac{1}{\sqrt{2}}\left[\left\{\epsilon_1(\omega)^2 + \epsilon_2(\omega)^2\right\}^{1/2} - \epsilon_1(\omega)\right]^{1/2}. \tag{6}$$

At low frequency ($\omega = 0$), we get the refractive index as

$$\eta(0) = \sqrt{\varepsilon_1(0)}. \tag{7}$$

This is called static refractive coefficient. The refractive index and extinction coefficient are further used in the following relation to evaluate normal incident reflectivity $R(\omega)$ of $CsPbI_3$:

$$R(\omega) = \frac{(\eta - 1)^2 + \kappa^2}{(\eta + 1)^2 + \kappa^2}. \tag{8}$$

Similarly, absorption coefficient $\alpha(\omega)$ and optical conductivity $\sigma(\omega)$ are calculated by the relations:

$$\alpha(\omega) = \frac{2\omega\kappa(\omega)}{c} \tag{9}$$

and

$$\sigma(\omega) = \frac{\alpha \eta c}{4\pi} \tag{10}$$

where c is the speed of light.

3. Results and discussion

3.1 *Electronic band structure and density of states*

The electronic behaviour of $CsPbI_3$ has been discussed in this section. The band structure and density of states (DOS) are calculated with well-converged self-consistent solution of plane-wave pseudopotential [23] shown in figure 3, which indicates a very small direct band gap at the symmetry point R, where the minimum of conduction band and the maximum of valence band are located. Fermi energy E_F lies near the conduction band. The value of energy band gap obtained in this work is 1.28 eV, which is in good agreement with the earlier reported data [24,25]. It can be seen from the band structure plot, that $CsPbI_3$ shows ionic characteristics. The nature of bonds in the band structure plot can be further elucidated by partial density of states (PDOS). The PDOS structure in figure 4 shows a small mixing of Pb-p and Cs-d with Cs-p states in the conduction band within the energy range 2.9–5.5 eV. It is also visible in the valence band that there is a small hybridization of I-p and Pb-p states in the range from -4 eV to -5.1 eV. This indicates the presence of weak covalent bonding between Pb and I and between Cs and Pb orbitals. There is strong ionic bonding between Cs and I orbitals [26,27]. In figure 4, we have observed dominating Pb-p states in the conduction band and I-p states in the valence band near Fermi level. In the energy range from -8 eV to -12 eV, Pb-s orbital electrons are seen and beyond -12 eV, I-s orbital electrons are seen with small contributions of Pb-p and Cs-d orbital electrons. The relative intensities of the peaks associated with Cs, Pb and I states are observed in our results (figure 4). The states of Cs atoms, i.e. Cs-s, Cs-p and Cs-d states, are present in the conduction band in the energy range 0.9–11.25 eV which shows that Cs has strong dominance in the higher energy range of the conduction band along with the Pb-p states [6,16]. The electronic states of cesium atom are highly localized in the valence and conduction bands and do not contribute to the states near Fermi level [28]. To show the ionic character of the compound, we have obtained the charge density distribution and displayed it in figure 5. The bonding is purely ionic for isolated charge density contours, whereas it is partly covalent if there exists any overlapping between cation/anion charge density contours [29]. In figure 5, we can see the isolated contours of Cs and I which clearly show the strong ionic nature of the compound. The electronegativity of I is 2.66 and Cs

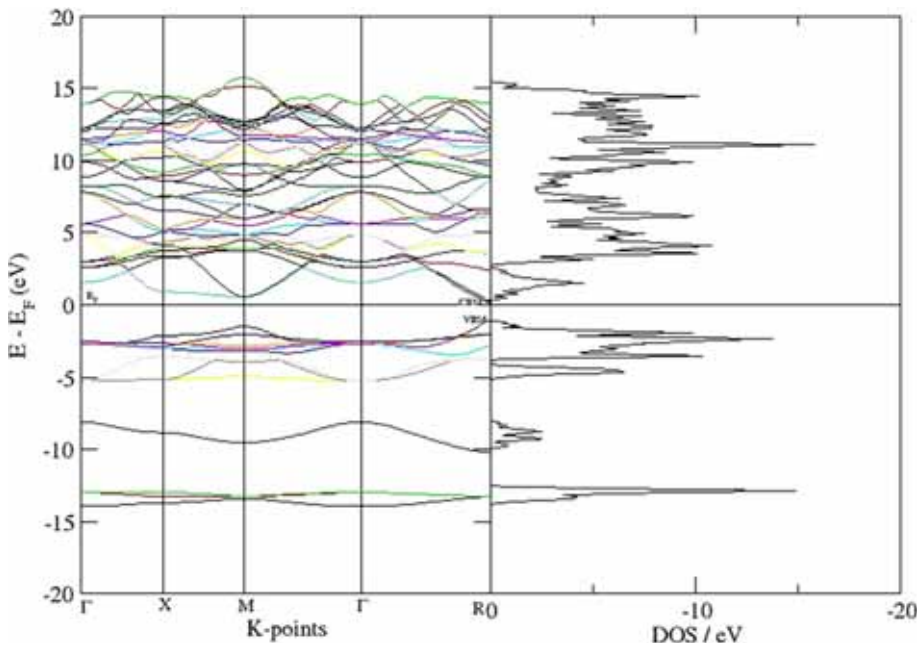

Figure 3. Band structure along high symmetry directions of the Brillouin zone of cubic $CsPbI_3$. The horizontal soild line corresponds to the Fermi energy (E_F) shifted to zero reference level. The positions of Γ, X, M, and R corresponds to $(0,0,0)$, $(0.5,0,0)$, $(0.5,0.5,0)$ and $(0.5,0.5,0.5)$. Minimum of conduction band (CBM) and maximum of valence band (VBM) are also shown in the band structure at R which implies a direct band gap. Total density of states of cubic $CsPbI_3$ is also shown along with the band structure.

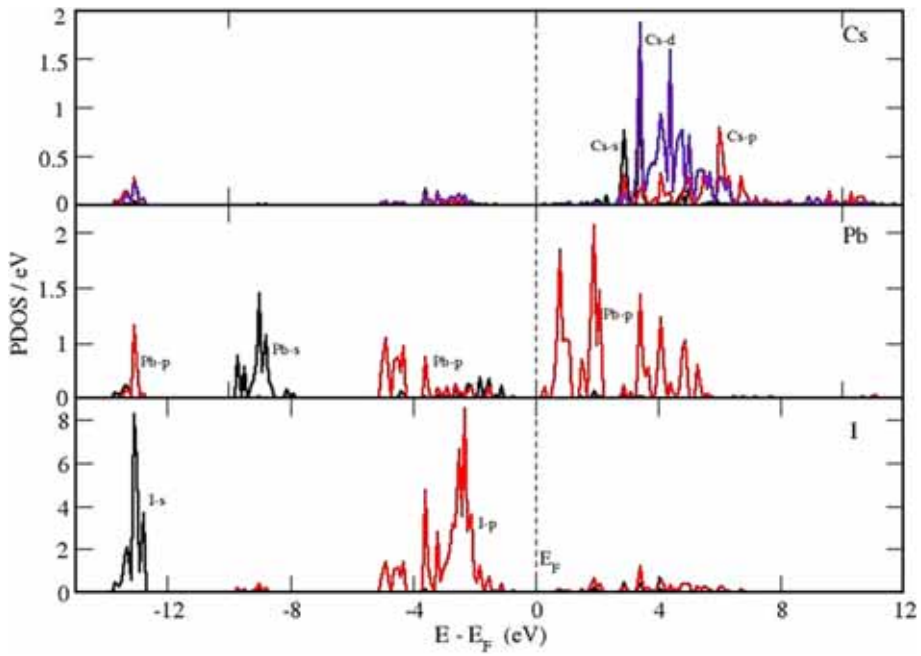

Figure 4. Partial density of states corresponding to Cs, Pb and I orbitals respectively showing the orbital character of the atoms of cubic $CsPbI_3$.

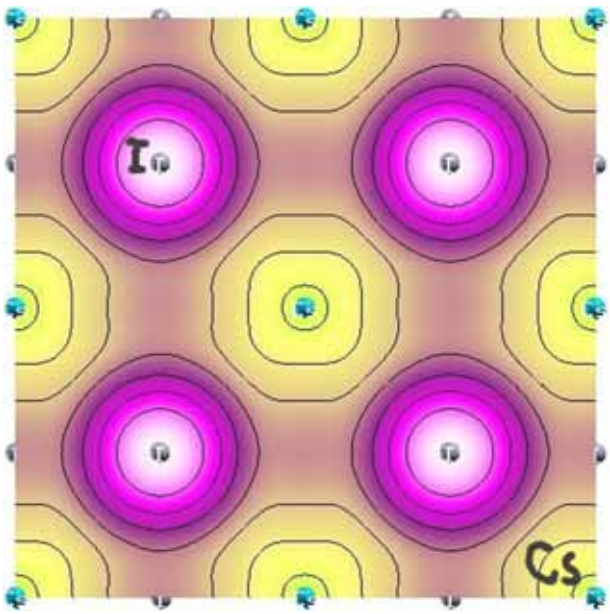

Figure 5. Total electronic charge density distribution of cubic $CsPbI_3$.

is 0.79 which provides the information of charge transfer from Cs to I, i.e. charge depletion will occur at Cs while accumulation takes place at I.

3.2 *Dielectric and optical properties*

The linear response of the crystal to the electromagnetic radiation is described by dielectric function $\varepsilon(\omega)$ [30]. The dielectric function $\varepsilon(\omega) = \varepsilon_1(\omega) + i\varepsilon_2(\omega)$ describes the optical response of the medium to the incident photons $E = \hbar\omega$. The imaginary part $\varepsilon_2(\omega)$ relates to the electronic band structure of the material and describes its absorptive nature [16]. Figure 6i shows that the critical point of the compound is 1.35 eV [6], which is in good agreement with the earlier reported data and it can be compared with the energy band gap of the material. There are four high peaks at 3.97 eV, 5.22 eV, 5.71 eV and 8.16 eV. Origin of these peaks lies in the interband transitions which can be related to partial DOS of the compound. The first peak arises due to the transition of electrons from I-*p* states of the valence band to the Pb-*p* states of the conduction band. Second and third peaks are due to the electron transition from I-*p* states of the valence band to Cs-*d* and Pb-*p* states in the conduction band. The last peak is due to the transition of electrons from Cs-*p* to Pb-*p* states [6]. Broad spectra of $\varepsilon_2(\omega)$ show high absorption in different regions of energy spectrum [27,31]. From the electronic band structure shown in figure 3, we get a small direct band gap (1.28 eV), which gives therefore high absorption [6]. In the inset of figure 6i, we have given the response of $\varepsilon_2(\omega)$ for the negative values of ω. Equation (2) implies that $\varepsilon_2(\omega')$ is an odd function, and from the inset of figure 6i, we conclude that this oddity will give $\varepsilon_2(0) = 0$. The real part of the dielectric function $\varepsilon_1(\omega)$ is shown in figure 6ii. The important parameter that can be obtained from this spectra is its zero frequency limit $\varepsilon_1(0)$, which is the electronic part of the static dielectric constant

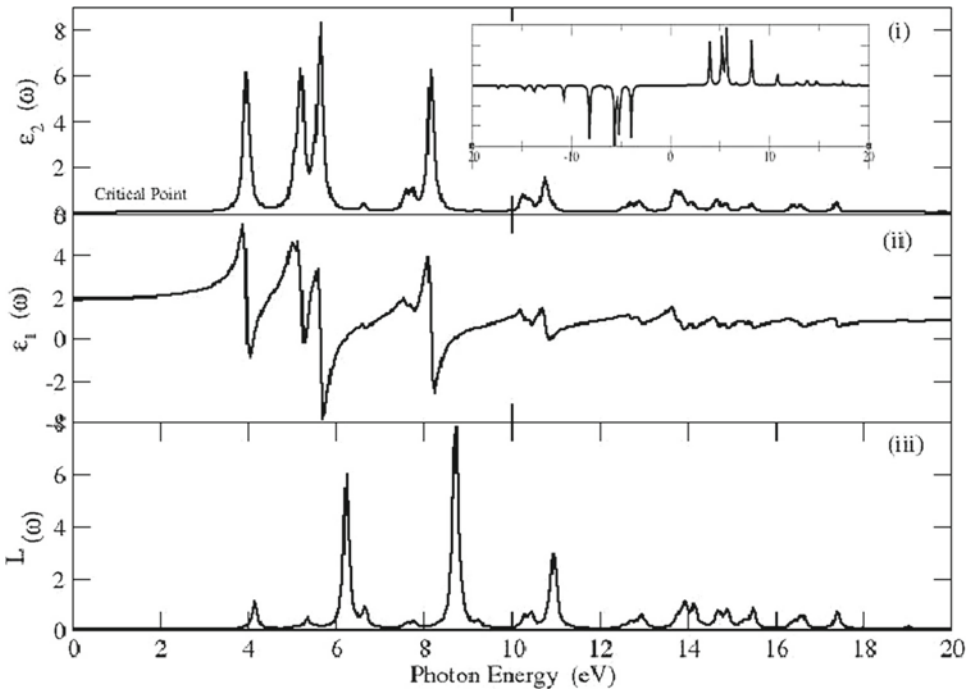

Figure 6. (**i**) Imaginary part, (**ii**) real part of dielectric function and (**iii**) energy loss as a function of energy for cubic $CsPbI_3$.

$\varepsilon_1(0)$. Figure 6ii shows that $\varepsilon_1(\omega)$ reaches a maximum value and then starts decreasing and in certain ranges it goes below zero. For negative value of $\varepsilon_1(\omega)$, materials show metallic nature [16,27]. The energy loss function $L(\omega)$ is determined from the experimental data of small scattering angles. From figure 6iii it can be seen that the spectra lie in the energy range corresponding to the electronic excitation of different orbitals. A broad band appears in the energy range 8.2–20 eV for the given material. This energy range lies in the low-loss region which corresponds to the interband transitions and plasmons losses. From eqs (1) and (4), we can relate the interband transitions obtained from $\varepsilon_2(\omega)$. These interband transitions can be further correlated with the energy loss spectrum shown in figure 6iii. A significant feature in the low-loss spectrum (<50 eV) is the bulk plasmon, which has the intensity of several orders of magnitude higher than core-loss edges due to collective oscillation of loosely bound electrons, which runs as a longitudinal wave through the volume of the crystal with a characteristic frequency. In this low-loss region, interband transitions and plasmon losses are observed. Plasmon losses correspond to the collective oscillation of the valence electrons and their energy is related with density of valence electrons. The plasmon is defined by the vanishing real part of the dielectric function and the minimum of the imaginary part. The plasmon energy (the maximum of the loss-function) is identified as occurring at the point where $\varepsilon_1(\omega)$ crosses zero with a positive slope. The plasmon frequency of the material obtained is 7.17 eV [22,27,32]. Refractive index $\eta(\omega)$ of a material determines the speed of light in the material. It is an important constant for optoelectronic devices as it would be responsible for the nature of interactions of the material with the optical energy incident on the material. The trend of $\eta(\omega)$ with photon energy can be seen in figure 7a. The value of $\eta(\omega)$ is determined by eq. (4). When the optical energy interacts with matter, it scatters and loss occurs. These losses are described by the extinction coefficient $\kappa(\omega)$. Its variation with photon energy is shown in figure 7b. The absorption coefficient $\alpha(\omega)$ is the property of a material which describes the absorption of light by it. The materials are classified as transparent, translucent and opaque according to the absorption strength of the material. For photoelectronic applications, $\alpha(\omega)$ is supposed to be an important factor. By plotting the graph between $(\alpha h\nu)^2$ vs. photon energy $(h\nu)$, direct optical band gap $E_g(\text{opt})$ is determined. The extrapolation of the straight line to $((\alpha h\nu)^2 = 0)$ provides the value of the band gap. The absorption coefficient as a function of optical energy is shown in figure 7d. Optical conductivity $\sigma(\omega)$ is a powerful tool for studying the electronic states of the materials. If a system is subjected to an external electric field, then a redistribution of charges occurs and currents are introduced [15,16,22]. The variation of $\sigma(\omega)$ as a function of photon energy is shown in figure 7e. The response of $\kappa(\omega)$ and $\alpha(\omega)$ is revealed from figures 7b

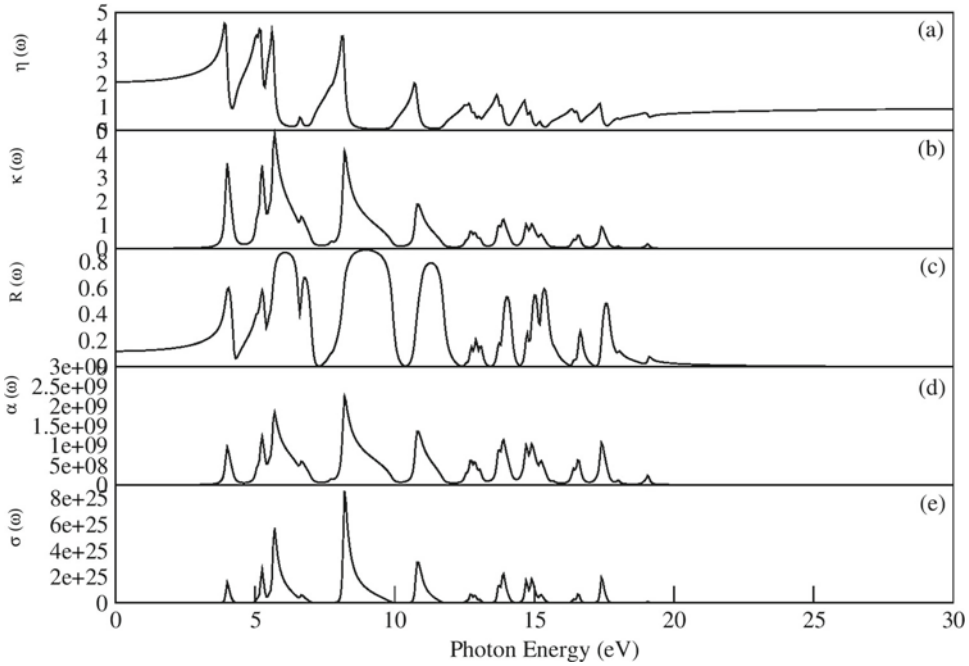

Figure 7. Photon energy-dependent optical parameters for cubic $CsPbI_3$.

Table 1. Electronic properties of cubic $CsPbI_3$ and optical properties at zero-frequency limit for cubic $CsPbI_3$.

Parameters	This work
$\varepsilon_1(0)$	4.13
β	128.12
η	2.03, (2.45) [6]
E_g (eV)	1.26, (1.07) [24], (1.73) [25], (1.3) [6]
E_g(opt) (eV)	1.35, (1.25) [6]
α_c (eV)	2.48
R_c (eV)	0.149, (0.177) [6]
κ_c (eV)	1.79
σ_c (eV)	3.53

and 7d. The zero-frequency values of both the variables are listed in table 1. These variables have strong response to the incident photons in the range 3.36–20 eV. From figure 7c, the zero-frequency limit of reflectivity $R(\omega = 0)$ for the compound is found to be 0.149. There are high reflection peaks at energies 6.108 eV, 8.95 eV and 11.35 eV corresponding to the negative values of $\varepsilon_1(\omega)$. The optical conductivity rises in response to the photon energy from 3.53 eV and its highest value is found at 8.20 eV. The critical value of $\sigma(\omega)$ and polarizability β is listed in table 1. An appreciable response of $\sigma(\omega)$ is found to be in the range 3.52–17.82 eV.

4. Conclusion

The electronic, dielectric and optical properties of cubic $CsPbI_3$ are studied using density functional plane-wave pseudopotential method. The band structure shows that the material is highly ionic. A strong ionic bond is observed between Cs–I states which is also clearly seen in the chemical bonding study and a weak covalent bond has been observed between Pb–I and Cs–Pb states on inspection of the partial density of states. From the direct band-gap and optical properties of cubic $CsPbI_3$ as a function of photon energy, it has been found that the compound absorbs light in the major portions of electromagnetic spectrum, i.e. ultraviolet (UV), visible and near-infrared (IR) regions. Thus, the compound can efficiently be used as coating material on optoelectronic materials. Furthermore, the authors are not aware of any published data of energy loss spectrum along with other photon energy-dependent optical properties of the compound. So, our work can be used to cover this lack of data of the compound.

Acknowledgements

The authors are thankful to Prof. Umesh V Waghmare from JNCASR, Bengaluru for the fruitful discussion and suggestion and Madhya Pradesh Council of Science and Technology (MPCST) for providing Fellowship for Training of Young Scientists (FTYS). The authors highly acknowledge all the learned referees for providing suggestions that have improved the scientific quality and presentation of the manuscript. Amreen Bano and Preeti Khare are thankful to University Grants Commission (UGC), New Delhi, for providing financial

assistance through Maulana Azad National Fellowship (MANF) and Dr D S Kothari Post-doctoral Fellowship respectively.

References

[1] S Moskvin, A A Makhnev, L N Nomerovannaya, N N Loshkareva and A M Balbashov, *Phys. Rev. B* **82**, 035106 (2010)
[2] C Weeks and M Franz, *Phys. Rev. B* **82**, 085310 (2010)
[3] N Mathur and P Littlewood, *Phys. Today* **56**, 25 (2003)
[4] S Liu, F Zheng, N Z Koocher, H Takenaka, F Wang and A M Rappe, *J. Phys. Chem. Lett.* **6**, 693 (2015)
[5] J H Heo, S H Im, J H Noh, T N Mandal, C-S Lim, J A Chang, Y H Lee, H-J Kim, A Sarkar, M K Nazeeruddin, M Gratzel and S Il Seok, *Nat. Photon.* **7**, 486 (2013)
[6] G Murtaza, I Ahmad, B Amin, A Afaq, M Maqbool, J Maqsood, I Khan and M Zahid, *Opt. Mater.* **33**, 553 (2011)
[7] M M Lee, J Teuscher, T Miyasaka, T N Murakami and H J Snaith, *Science* **338**, 643 (2012)
[8] J Burschka, N Pellet, S-J Moon, R Humphry-Baker, P Gao, M K Nazeeruddin and M Gratzel, *Nature* **499**, 316 (2013)
[9] N Pellet, P Gao, T Y Yang, M K Nazeeruddin, J Maier and M Gratzel, *Angew. Chem. Int. Ed. Engl.* **53**, 3151 (2014)
[10] J H Noh, S H Im, J H Heo, T N Mandal and S Il Seok, *Nano Lett.* **13**, 1764 (2013)
[11] C R Kagan, D B Mitzi and C D Dimitrakopoulos, *Science* **283**, 945 (1999)
[12] H Klauk, *Phys. World* **13**, 18 (2000)
[13] P Giannozzi, S Baroni, N Bonini, M Calandra, R Car, C Cavazzoni, D Ceresoli, G L Chiarotti, M Cococcioni, I Dabo, A Dal Corso, S Fabris, G Fratesi, S de Gironcoli, R Gebauer, U Gerstmann, C Gougoussis, A Kokalj, M Lazzeri, L Martin-Samos, N Marzari, F Mauri, R Mazzarello, S Paolini, A Pasquarello, L Paulatto, C Sbraccia, S Scandolo, G Sclauzero, A P Seitsonen, A Smogunov, P Umari and R M Wentzcovitch, *J. Phys.: Condens. Matter* **21**, 395502 (2009)
[14] J P Perdew and Alex Zunger, *Phys. Rev. B* **23**, 5048 (1981)
[15] R Khenata, M Sahnoun, H Baltache, M Rerat, A H Rashek, N Illes and B Bouhafs, *Solid State Commun.* **136**, 120 (2005)
[16] K E Babu, N Murali, K V Babu, P T Shibeshi and V Veeraiah, *Acta Phys. Pol. A* **125**, 1179 (2014)
[17] Ph Ghosez, X Gonze and J-P Michenaud, *Ferroelectrics* **206**, 205 (1998)
[18] R Terki, H Feraoun, G Bertrand and H Aourag, *Phys. Status Solidi B* **242**, 1054 (2005)
[19] H S Kim, C R Lee, J H Im, K B Lee, T Moehl, A Marchioro, S J Moon, R Humphry-Baker, J H Yum, J E Moser, M Gratzel and N-G Park, *Sci. Rep.* **2**, 591 (2012)
[20] K Miura, M Azuma and H Funakubo, *Materials* **4**, 260 (2011)
[21] Ph Ghosez, E Cockayne, U V Waghmare and K M Rabe, *Phys. Rev. B* **60**, 836 (1999)
[22] S Saha, T P Sinha and A Mookerjee, *Phys. Rev. B* **62**, 8828 (2000)
[23] B Xu, X Li, J Sun and L Yi, *Eur. Phys. J. B* **66**, 483 (2008)
[24] R A Jishi, O B Ta and A A Sharif, arXiv:1405.1706v2 (2014)
[25] R E Beal, D J Slotcavage, T Leijtens, A R Bowring, R A Belisle, W H Nguyen, G Burkhard, E T Hoke and M D McGehee, *J. Phys. Chem. Lett.* **1** (2016), DOI:10.1021/acs.jpclett.6b00002
[26] Hayatullah, G Murtaza, S Muhammad, S Naeem, M N Khalid and A Manzar, *Acta Phys. Polon. A* **124**, 102 (2013)
[27] L Lang, J-H Yang, H-R Liu, H J Xiang and X G Gong, *Phys. Lett. A* **378**, 290 (2014)
[28] M Afsari, A Boochani and M Hantezadeh, *Optik – Int. J. Light Electron Opt.* **127**, 11433 (2016)
[29] N Acharya, B Fatima and S P Sanyal, *J. Phys. Chem. Solids* **99**, 25 (2016)
[30] S D Mo and W Y Ching, *Phys. Rev. B* **51**, 13023 (1995)
[31] M Maqbool, I Ahmad, H H Richardson and M E Kordesch, *Appl. Phys. Lett.* **91**, 193511 (2007)
[32] A Mamedov, S Güngör and S Çabuk, *J. Electron. Spectrosc. Relat. Phenom.* **79**, 75 (1996)